JCTC Journal of Chemical Theory and Computation

Article

pubs.acs.org/JCTC

Ab Initio Treatment of Bond-Breaking Reactions: Accurate Course of HO_3 Dissociation and Revisit to Isomerization

A. J. C. Varandas*

Departamento de Química, Universidade de Coimbra, 3004-535 Coimbra, Portugal

Supporting Information

ABSTRACT: An efficient scheme is devised for accurate studies of bond-breaking/forming reactions and illustrated for HO_3. It is suggested and numerically demonstrated that an accurate dissociation path for the title system can be obtained by defining the central OO bond as the reaction coordinate. The approach consists of optimizing the dissociation path at the full-valence-complete-active space level of theory followed by single-point multireference configuration interaction calculations along it. Using large diffusely augmented basis sets of the correlation consistent type, accurate dissociation curves are then obtained for both the *cis*- and *trans*-HO_3 isomers by extrapolating the calculated raw energies to the complete basis set limit. The profiles show a weak van der Waals type minimum and a small barrier, both lying below the dissociation asymptote. It is shown that this barrier arises at the break-off of the central OO chemical bond and onset of the OH···O_2 hydrogen bond. The calculated dissociation energies (D_e) are 4.5 ± 0.1 and 4.7 ± 0.1 kcal mol^{-1} for the *cis*- and *trans*-HO_3 isomers, respectively, with a very conservative estimate of the dissociation energy (D_0) for *trans*-HO_3 being 2.7 ± 0.2 kcal mol^{-1} and a more focused one being 2.8 ± 0.1 kcal mol^{-1}. This result improves upon our previous estimate of this quantity while overlapping in the lower range of 2.9 ± 0.1 kcal mol^{-1}, the commonly accepted value from the low-temperature CRESU experiments. Since the *cis*-HO_3 isomer is predicted to be 0.15 kcal mol^{-1} less stable than *trans*-HO_3, this may partly explain the failure to obtain a clear characterization of the former. The isomerization (torsional) potential is also revisited and a comparison presented with a curve inferred from spectroscopic measurements. Good agreement is observed, with the accuracy of the new calculated data commending its use for the reanalysis of the available vibrational−rotational spectroscopic data.

1. INTRODUCTION

Radical−radical reactions are critically important in atmospheric chemistry and combustion processes, both areas of major practical and social relevance. They cover the recombination of two radicals to form a new bond, and the rupture of a bond in a molecule to form radicals. Such processes offer an enormous challenge in *ab initio* electronic structure theory since calculations require multireference methods which are known to scale dramatically with system size [i.e., number of electrons N and number of one-particle states (orbitals) n for a desired multiplicity $(2S + 1)$] and hence are unaffordable for all but small systems.

Paradigmatic among the methods appropriate for dealing with radical−radical reactions is the multireference configuration interaction (MRCI) method where, exploiting symmetry, Slater determinants are first linearly combined to make the reference functions be eigenfunctions of the total spin angular momentum $\hat{S}^2$ (configuration state functions, CSFs). Not surprisingly, the number of CSFs easily grows exponentially large,[1] with the full CI expansion becoming of extremely large dimensions for even a small number of electrons with a modest orbital basis size. Thus, the MRCI method becomes essentially unaffordable for most systems of practical relevance. The expansion must therefore be severely truncated, normally at double excitations, with approximate methods having to be devised to deal with large systems even at the simplest but highly expensive MRCISD (denoted heretofore as MRCI) expansion so obtained. Regrettably, truncated CI methods suffer from a lack of size extensivity at any level of truncation. Fortunately, there are methods capable of mitigating such a deficiency. Among the more recent approaches, one should mention, e.g., the CISD[TQ] method,[2] which includes higher-excitation effects by partitioning the orbital space according to the importance of the orbitals; the MRCISD(TQ) and nR-MRCISD(TQ) methods[3,4] that introduce a noniterative correction to MR-CISD energies to account for the effects of higher excitations; and the CEEIS method[5] for extrapolating the higher excitations using intrinsic scaling techniques (a recent review that discusses the latest developments in the *ab initio* CI methodology can be found elsewhere[6]). As discussed later, the lack of size extensivity can also be attenuated *a posteriori* by including the popular Davidson correction (+Q) that approximately corrects for quadruple electronic excitations as adapted to the MRCI approaches.[7,8]

A very convenient and frequently used reference for the MRCI expansion is the full-valence complete-active-space (FVCAS) wave function. Nominally a full CI (FCI) expansion in the valence space, this makes the method "black box" in nature and hence easy to use. The internal (valence) and external orbitals assume then the role of occupied and virtual orbitals in an FVSCF calculation, with the internal and external orbitals being mixed among each other until the optimum internal orbitals are found. Because the active orbital space coincides with the true valence space, the correct dissociation at all limits is automatically guaranteed, although there may be

Received: September 7, 2011
Published: January 5, 2012

   dx.doi.org/10.1021/ct200773b | *J. Chem. Theory Comput.* 2012, 8, 428−441

many configurations included which are completely unimportant.[9]

Of particular relevance in the atmospheric context[10] is the title radical and its stability relative to dissociation by rupture of the central bond, namely $O_aO_bO_cH \rightarrow O_aO_b + O_cH$. A major goal of the present work is to suggest an efficient (cost-effective) scheme to obtain a fully optimized MRCI-like dissociation curve. It is based on the following four-point premise (or simply premise):

1. Electronic structure calculations of bond-breaking/forming processes are best treated by MRCI methods, preferably when the Davidson correction (MRCI+Q) is added.
2. A convenient reference for the MRCI expansion is the FVCAS wave function since it warrants the correct description of the dissociation process at all possible asymptotes while making a clear partition of the static and dynamical correlation.
3. Bond-forming/breaking processes are well described (qualitatively, sometimes even quantitavely) at the FVCAS level of theory by choosing an active bond (O_bO_c in the present case) and optimizing all other degrees of freedom at each point of a predefined grid of values of the active bond coordinate that is kept inactive during the optimization procedure.
4. The dissociation path can be accurately obtained by performing single-point MRCI and MRCI+Q calculations at the grid of geometries of the active coordinate (O_bO_c) so defined.

Although the above scheme or variants thereof[11,12] has been used before to carry out MRCI calculations, to our knowledge it has not been tested or justified in a sense as detailed as presented here. Indeed, the algorithm based on it may encounter a similarity on the well-established approach to closed-shell interactions whereby the fully correlated potential energy curve or surface (PES) is obtained by adding the dynamical correlation to the near Hartree−Fock (HF) part. More specifically, for a closed-shell interaction between molecules A and B, the intra-atomic coordinates would be optimized at the HF level of theory at each A−B separation while the whole PES would be obtained by adding the dynamical correlation to the HF PES optimized by keeping the intermolecular bond distance fixed at each point of a predefined grid of values. The method is then based on the assumption that a correct diagnostic is made of the bond that is broken/formed, with the remaining part of the molecule being treated as a spectactor optimally described at the FVCAS level of theory. The subject will be elaborated further in the Results and Discussion section, where the above premise is shown to perform accurately for the title system. We also revisit recent work[13] on the isomerization (torsional) PES by performing further accurate MRCI calculations on the path that connects the *cis*- and the *trans*-HO_3 isomers. A comparison with the most recent experimental and theoretical work on the torsion potential[14] of HO_3 will then be presented.

1.1. A Brief Survey on the HO_3 System. The first direct observation of HO_3 goes back to 1999[15] using neutralization−reionization mass spectrometry, followed by its infrared observation in Ar and H_2O-ice matrices.[16] Observations of rotational transitions of HO_3 and DO_3 in the gas phase were more recently reported[17] using Fourier-transform microwave (FTMW) spectroscopy. The determined rotational constants, as well as the ratio of a-type and b-type transition intensities, have been found to be consistent with a *trans* planar structure of $^2A''$ character (no *cis* conformer had yet been observed). With the help of data from MRCI calculations with a triple-ζ augmented correlation consistent basis set[18] (these functions belong to Dunning's basis-set family denoted as aug-cc-pV*X*Z or AV*X*Z, where $X = T$ is the cardinal number), Suma et al.[17] utilized the A and B rotational constants to determine an equilibrium geometry by assuming a planar *trans* geometry and bond lengths for HO_c and O_aO_b fixed at their *ab initio* values. One should recall that the structures obtained by microwave spectroscopy are not equilibrium structures that are directly comparable to those determined from quantum chemistry, with the extraction of an equilibrium structure from microwave data being virtually impossible. The above led to a prediction of 1.688 Å for the O_bO_c bond length.[17] Such a long central OO bond distance has also led to the suggestion[19] that it would not be truly covalent. Furthermore, such an untypical length created excitement because accurate single-reference coupled-cluster (CC) type methods predict it to be much shorter. In addition, the stability of HO_3 relative to dissociation into the ground state fragments, $OH(X^2\Pi) + O_2(X^3\Sigma_g^-)$, became open to debate. Note that the presence of HO_3 in measurable concentrations in Earth's atmosphere depends on the equilibrium $HO_3 \rightleftharpoons O_2(X^3\Sigma_g^-) + OH(X^2\Pi)$ and hence on how stable it really is.[20−22]

A full assessment of the atmospheric abundance of the HO_3 radical requires a detailed knowledge of its thermochemical properties. The first experimental measurements are due to Speranza,[23] who inferred an enthalpy of formation of -1 ± 5 kcal mol^{-1} and an O_bO_c bond dissociation enthalpy of 10 ± 5 kcal mol^{-1}. More recently, Lester and co-workers[20,21,24,25] utilized infrared action spectroscopy to measure the OH product state distribution that is observed from the vibrational predissociation of HO_3 and predicted from the energetically highest observed OH product channel an upper limit for the dissociation energy of the O_bO_c bond at 0 K (D_0) of 6.12 kcal mol^{-1}. Use of the DO_3 isotopomer allowed[21] a further reduction of the upper limit to 5.31 kcal mol^{-1}. Better estimates could have been obtained if accurate zero-point energies (ZPEs) for HO_3 and DO_3 were available, an issue that will be a focal point of our discussion later.

The literature on HO_3 is vast[10,13,14,17,19−23,25−33] (a more complete account can be found in our[13] and other such reports by cross referencing). Theoretically, the first study on the HO_3 radical goes back to the work by Blint and Newton[34] in 1973 when discussing interoxygen bonding in a series of H_xO_y compounds ($x = 0, 1, 2$; $y = 2, 3$). Such a work focused on both the structural and dynamical aspects of the nature of HO_3. First, the work focused on its structure, to investigate whether it would be planar and, if so, whether both the *cis* and *trans* isomers would be stable. Particular attention has subsequently been paid to whether the long O_bO_c bond length inferred from the experiments of Suma et al.[17] could be reproduced. Second, research has been carried out on the dynamics of both $H + O_3$ and $O + HO_2$ reactions[35] (see also references therein), and more recently on the strength of the $HO-O_2$ bond and its implications on the kinetics of the bond-breaking/forming reactions $HO_3 \rightleftharpoons HO + O_2$ in the context of atmospheric chemistry. Suffice it to say in this respect that, despite being a four-atom species, the calculation of an accurate global PES for ground-state HO_3 remains an overwhelming task.[30] Recently,[12,13] we have utilized a cost-effective scheme based on

the extrapolation to the complete basis set (CBS) limit of accurate *ab initio* calculations to study the HO_3 optimum torsional path connecting the *cis* and *trans* isomers. Although predictions have sporadically appeared in the literature showing that the *trans*-HO_3 isomer is more stable than *cis*-HO_3, to our best recollection, our own has been the first to systematically demonstrate a stability ordering in good agreement with the experimental[14] evidence (which has been published independently and almost simultaneously).

In subsequent work, we have suggested a similar strategy to determine the minimum energy path for dissociation of the title radical into OH + O_2 ground-state products. The agreement between the value of dissociation energy D_0 (obtained after subtraction of the zero-point energy correction, ΔE_{ZPE}, from the classical dissociation energy, D_e) estimated from our calculations with the recent result inferred from the CRESU experiments by Le Picard et al.,[22] 2.4 ± 0.1 vs 2.9 ± 0.1 kcal mol^{-1}, is also good, but the difference left enough margin for questioning its origin and suggesting an even more accurate analysis of the subject. A major goal of the present work is therefore to examine in detail the issue of stability of HO_3, and the dissociation reaction $HO_3 \rightarrow OH + O_2$, by using the four-point premise stated at the Introduction.

Recent theoretical estimates of D_0 in the *trans*-HO_3 conformer cluster around[20] 1 to 3 kcal mol^{-1}, thus considerably below the above experimental upper bound of 5.31 kcal mol^{-1}. An exception to this is density functional theory calculations[32] based on the HCTH functional with the AV*T*Z basis set, which predict a D_0 of 6.15 kcal mol^{-1}. Unfortunately, they imply an O_bO_c bond length of 1.610 Å for *trans*-HO_3, a value significantly shorter than the commonly accepted one of 1.688 Å. The situation of D_0 now seems settled with Le Picard's et al.[22] value of 1030 ± 30 cm^{-1} [2.9 ± 0.1 kcal mol^{-1}], even if further analysis is welcome.

As noted above, a major difficulty in obtaining D_0 stems from the lack of an accurate ZPE value for HO_3. While the ZPEs of the diatomic fragments can be calculated very precisely from well characterized spectroscopic constants, for polyatomic molecules, calculation of ZPE requires knowledge of the harmonic vibrational frequencies as well as the anharmonicities and a constant term which is often not considered but can be sizable (up to some 100 cm^{-1} or so for molecular species with large rotational constants such as HO_3).[36−39] Being generally not known, the obvious step[14] is *ab initio* electronic structure calculations. However, theoretical methods that reliably describe bond-breaking/forming processes besides allowing for harmonic/anharmonic frequency analysis are essentially unaffordable for the title hydroxyl-peroxy radical. Varner et al.[20] predicted a correction of ΔE_{ZPE} = −2.33 kcal mol^{-1} when based on the harmonic formula and observed fundamental frequencies for *trans*-HO_3, while the result calculated from their own second-order vibrational perturbational analysis yielded ΔE_{ZPE} = −2.74 kcal mol^{-1}. Beames et al.[14] highlighted the criticality of the situation on obtaining accurate partition functions by explicitly considering their torsional potential. Yet, their calculations still bare assumptions: the torsional mode (ν_1) is treated as separable from the remaining five modes (ν_2 to ν_6), and modes ν_2 to ν_6 are considered as harmonic. Furthermore, they assumed that the rotational constants were those known for the *trans* conformer.[17] While their results have shown that the HO_3 partition function calculated at 300 K can be up to a factor of 3 or so larger than the value obtained from the harmonic treatment, the predicted dissociation energy of D_0 = 1004 ± 24 cm^{-1} lies within the uncertainty of the value from the CRESU experiments.[22] However, as Beames et al.[14] have also observed, models that consider anharmonicity in other modes and/or contributions from quasibound states above the dissociation limit[40,41] would increase further the magnitude of the HO_3 partition function and decrease D_0. Additionally, they have stressed[14] that the influence on the partition function can be relatively small compared to that on the dissociation energy.

2. METHODOLOGY

Extensive theoretical work employing a variety of methods and basis sets has recently been carried out by the author[13] on the isomerization of the title radical in its ground $^2A''$ electronic state (in C_s symmetry). There as well as in a recent calculation of the dissociation curve[12] and the study here reported, only correlation consistent basis sets[18,42,43] of the cc-pV*X*Z and aug-cc-pV*X*Z types (V*X*Z and AV*X*Z for brevity) as available in the EMSL[44] library have been utilized since they are specially adequate for quantitative work. Specifically, we have here conducted further high level MRCI calculations both including and without the inclusion of the Davidson correction[7,8] for values of the O_bO_c distance varying from 1.4 to 10 Å, with the largest distance taken as the separated products. All calculations employed the internally contracted MRCI[45,46] method as implemented in the Molpro[8] package, with the active space formed by all valence orbitals such as to warrant the correct behavior up to dissociation. Because their computation can be extremely demanding, core effects have been ignored. Specifically, the three lowest molecular orbitals have been treated as inactive, which yields 51 660 CSFs for the CAS reference wave function out of the 13 active orbitals (10*a*′,3*a*″). The MRCI included therefore three core orbitals, which yields a total of 92 431 012 contracted configurations with the AV5Z basis. At this level of theory, a geometry-optimization followed by harmonic vibrational frequency and normal mode calculations can take several weeks of uninterrupted work on a 64 bit double-core double-processor at 1.87 GHz even with the V*D*Z basis. Note that single-reference calculations[13] have shown that ignoring the core effects has no drastic consequences, which may be due to the fact that the calculations are restricted to valence regions of the PES. The above may also explain our use of convergence thresholds kept at or assuming values only somewhat tighter than the default,[8] except in a few cases (with the V*D*Z basis where values of 10^{-6} E_h $Å^{-1}$ and 1 μE_h were utilized for the gradient and energy).

Regarding the construction of the $HO_3 \rightarrow O_2$ + OH dissociation path, energies have been calculated along the O_bO_c coordinate with all degrees of freedom optimized at the CAS(19,13)/AV*Q*Z level of theory but keeping the O_bO_c distance fixed at each of the 29 distinct values that were chosen to do its mapping. Although this last point is taken as the dissociation limit, test calculations up to 100 Å have shown that the error is only ∼2 cal mol^{-1} for the AV5Z basis. The reported dissociation energies may then be underestimated by a few cal mol^{-1} (or K), an error that is considered to be negligible for most practical purposes. A convergence typically beyond the threshold values utilized in Molpro (often 10^{-6} E_h $Å^{-1}$ in the gradient) has been warranted at most values of the inactive coordinate except at the region where a rapid change of relative orientation of the fragments is expected, namely when passing from a valence regime to another dictated by long-range forces of the electrostatic, induction, and dispersion types.

dx.doi.org/10.1021/ct200773b | J. Chem. TheoryComput. 2012, 8, 428−441

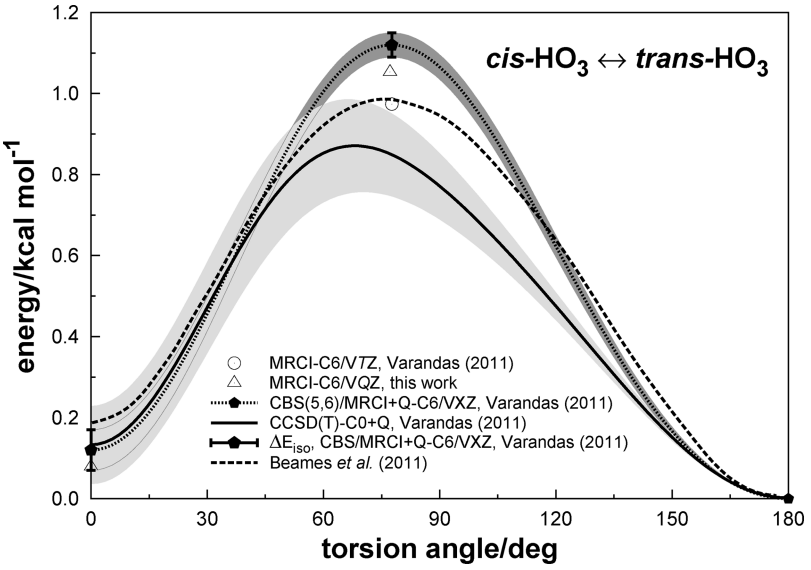

Figure 1. A comparison of our predicted theoretical curves at all-electron CBS/CCSD(T) and valence-only CBS/MRCI+Q levels of theory with the equation of motion coupled cluster results that have been scaled[14] such as to reproduce the observed torsional levels. The shaded areas indicate the estimated error margins.[13] See also, refs 13 and 59 for notation, and Table 1 of the SI for the MRCI+Q/VTZ value of ΔE_{iso}, which is not shown in the plot due to being negative.

For enhanced accuracy, the two contributions that make up the electronic energy [complete-active-space self-consistent field (CASSCF or CAS for brevity[47]) and dynamical correlation (dc)] have been separately extrapolated to the complete basis set (CBS) limit from the calculations here reported with the AV*X*Z basis, $X = D, T, Q, 5$. Thus, they complete recent work,[12] which employed the smaller V*X*Z basis set with cardinal numbers up to $X = 6$; these results will also be addressed in detail in the present work. For the CAS component, the two-parameter extrapolation formula of Karton and Martin[48] (KM; see also the paper by Jensen[49]) has been employed because the basis set convergence of the uncorrelated CAS energies (lacking dynamical correlation) is expected[50] to be comparable to that of HF energies for which it has been originally[48,49] suggested. In fact, when extrapolating from the two highest affordable bases, CBS(5,6)/CAS, the results obtained from the KM approach are found to compare nicely with the ones obtained from our own hybrid scheme[50] that employs the popular three-point exponential formula.[51,52] For the dc contribution, our own two-parameter uniform singlet- and triplet-pair extrapolation[50] (USTE) protocol has been utilized, with the CBS extrapolation carried out from the calculations with the two highest affordable bases (see elsewhere[53] for an early related development). Besides performing with high accuracy when compared with available explicitly correlated results, especially in cases where bases with high cardinal numbers are affordable, an asset of USTE is that reliable extrapolations are obtained even when *X* values as small as *T* and *Q* (often *D* and *T*) are utilized.[54−56] When both energy components employ the same pivotal cardinal numbers for the extrapolation, say X_1 and X_2, the CBS energies can be unambiguously labeled by indicating CBS(X_1,X_2), which is not the case here. Besides the core correlation effects, relativistic and spin−orbit corrections have also been neglected since they too have been found to play a minor role.[20] In addition, the basis set superposition error (BSSE) has been ignored[57,58] due to the CBS extrapolation of the energy having been performed.

3. RESULTS AND DISCUSSION

3.1. Isomerization Potential Revisited. Gathered in Table 1 of the Supporting Information (SI) are the geometries and energies of the stationary points predicted at valence-only MRCI and MRCI+Q levels of theory. The corresponding MRCI frequencies for affordable cases (including some to be described later) are reported in Table 2 of the SI. A first observation is that the optimizations have been carried out at the MRCI level of theory, and hence the structural parameters may differ slightly from those that would be obtained using MRCI+Q. This is particularly so for the O_bO_c bond distance, which tends to be shortened slightly when the Davidson correction is included. A remark should also be made on the MRCI+Q/V*D*Z results which show a rather long O_bO_c bond distance. We are not aware of any other estimates at this level of theory. However, the predicted values exceed by more than 1 Å the corresponding value of 1.472 Å in the *trans*-HO_3 isomer reported by Braams and Yu[32] at the MRCI//CAS(13,10) level. Since this has been fully optimized at the CAS(13,10) level, such a difference is tentatively attributed to the nonparallelism of the MRCI and CAS(13,10) energy landscapes along the central OO bond distance. In fact, a calculation of the vibrational frequencies has shown that the *cis*-HO_3 geometry corresponds actually to a saddle point with a low imaginary vibrational frequency of 24.31 cm^{-1}. Conversely, the *trans* isomer is a minimum but with a low vibrational frequency of 34.26 cm^{-1}. Both stationary points have been converged up to a gradient of 10^{-6} E_h $Å^{-1}$. At the MRCI+Q/V*T*Z level of theory, the significant observation from Table 1 of the SI is the fact that *cis*-HO_3 is predicted to be more stable than *trans*-HO_3 by −0.102 kcal mol^{-1}. However, the exothermicity ΔE_{iso} (= *cis*−*trans* energy difference) becomes positive when a V*Q*Z basis is used, now by 0.128 kcal mol^{-1}. This value can be compared with the one obtained by CBS extrapolation of single-point MRCI+Q calculations at the optimum *cis*-HO_3 and *trans*-HO_3 geometries obtained at the triple-ζ level. The results show that the stability of the *trans* isomer is enhanced relative to *cis*-HO_3 by $\Delta E_{iso} = 0.12 \pm 0.05$ kcal mol^{-1}, where a fairly conservative

dx.doi.org/10.1021/ct200773b | J. Chem. TheoryComput. 2012, 8, 428−441

Table 1. A Comparison of Fully Optimized Structures for HO_3 at the MRCI/VXZ//MRCI/VXZ Level of Theory with the Values Obtained by Performing Single-Point Calculations at the Optimized CAS/VXZ Geometry Keeping the O_bO_c Distance Inactive at the MRCI/VXZ//MRCI/VXZ Optimized Value[a]

		cis			*trans*		
X	property	opt MRCI	opt CAS	Δ	opt MRCI	opt CAS	Δ
D	$R_{O_aO_b}$	1.2185	1.2208	−0.0023	1.2163	1.2187	−0.0024
	$R_{O_bO_c}$	2.5426	2.5426	*b*	2.4723	2.4723	*b*
	R_{O_cH}	0.9794	0.9824	−0.0030	0.9789	0.9820	−0.0031
	$\angle O_aO_bO_c$	115.69	117.26	−1.57	113.77	113.29	0.48
	$\angle O_bO_cH$	84.44	87.68	−3.23	84.99	87.01	−2.02
	E(CAS)	−0.1292775	−0.1293106	0.0208	−0.1296677	−0.1296908	0.0145
	E(MRCI)	−0.5139023	−0.5138693	−0.0207	−0.5144220	−0.5143980	−0.0148
	E(MRCI+Q)	−0.5475417	−0.5475121	−0.0186	−0.5480451	−0.5480318	−0.0084
T	$R_{O_aO_b}$	1.2443	1.2515	−0.0072	1.2203	1.2276	−0.0073
	$R_{O_bO_c}$	1.5805	1.5805	*b*	1.6951	1.6951	*b*
	R_{O_cH}	0.9709	0.9766	−0.0057	0.9684	0.9744	−0.0060
	$\angle O_aO_bO_c$	111.96	111.94	0.02	110.48	110.64	−0.16
	$\angle O_bO_cH$	96.21	96.82	−0.61	95.03	94.95	0.01
	E(CAS)	−0.1868799	−0.1869647	0.0532	−0.1884282	−0.1885191	0.0570
	E(MRCI)	−0.7100383	−0.7099512	−0.0546	−0.7100288	−0.7099348	−0.0590
	E(MRCI+Q)	−0.7633563	−0.7633245	−0.0200	−0.7631942	−0.7631538	−0.0255
Q	$R_{O_aO_b}$	1.2388	1.2492	−0.0104	1.2150	1.2253	−0.0103
	$R_{O_bO_c}$	1.5767	1.5767	*b*	1.6909	1.6909	*b*
	R_{O_cH}	0.9690	0.9752	−0.0062	0.9665	0.9731	−0.0066
	$\angle O_aO_bO_c$	112.03	112.00	0.03	110.50	110.68	−0.18
	$\angle O_bO_cH$	96.51	97.00	−0.49	95.34	95.11	0.23
	E(CAS)	−0.2041251	−0.2042652	0.0879	−0.2059526	−0.2061102	0.0989
	E(MRCI)	−0.7711895	−0.7710448	−0.0908	−0.7713930	−0.7712332	−0.1002
	E(MRCI+Q)	−0.8302480	−0.8301867	−0.0385	−0.8303658	−0.8302817	−0.0528

[a]Geometries in angstroms and degrees. Energies in hartree (after adding 225 E_h to the total energy), except when referring to differences Δ*E* (defined as opt MRCI − opt CAS), which are given in kcal mol^{-1}. [b]Kept fixed at the MRCI/VXZ//MRCI/VXZ optimized value in this table (third or sixth column).

error bar has been assigned in order to encompass all CBS/MRCI estimates.[12]

A comparison of the calculated CBS/MRCI+Q/VXZ isomerization potential[13] with the curve inferred from the measurements of Beames et al.[14] is shown in Figure 1. Also shown is the curve obtained[13] with the coupled-cluster method including the perturbative triples correction [CCSD(T)/VXZ and CCSD(T)/AVXZ] once CBS extrapolated and added a value of 0.25 kcal mol^{-1} to account for the effect of triple and quadruple excitations[20,59] (with a VTZ basis set), which yields an exothermicity for the isomerization process of ΔE_{iso} = 0.14 ± 0.08 kcal mol^{-1}. Clearly, the agreement with the semiempirical curve[25] is good. Specifically, our results on the optimized torsional potential reveal a shape and isomerization barrier height similar to the equation-of-motion coupled-cluster (CC) curve which has been scaled[14] by a factor of 1.35 from a fit of the calculated torsion levels to the ones observed via infrared action spectroscopy.[25] Also indicated is the calculated valence-only MRCI+Q/VTZ barrier height. Although its value falls essentially over the semiempirical curve,[14] this may be a somewhat coincidental result since the agreement does not extend to both the optimum MRCI+Q/VQZ value of ΔE_{iso} and torsional barrier here calculated (shown by the triangles). Moreover, CBS extrapolation has not been done. Unfortunately, force calculations to characterize fully the saddle point for torsion at the MRCI/VQZ level of theory would take several months of uninterrupted computational time, and hence only a partial optimization of the geometry has been done, as indicated in Table 1 of the SI. As seen, these geometrical parameters differ little from the optimized MRCI/VTZ ones previously reported,[13] although the energetics are in significantly better agreement with the CBS/MRCI+Q prediction.

3.2. Dissociation Path. *3.2.1. Numerical Test of the Proposed Calculation Scheme.* Let us first address the issue of reliability of the four-point premise suggested earlier in the paper. Table 1 compares the geometries and energies calculated by using it (denoted as opt-CAS) with the values obtained by direct optimization at the MRCI level (opt-MRCI). The deviations are indicated under the heading of Δ. As shown, the opt-CAS energies are accurate up to a few hundredths of a kcal mol^{-1}. Similarly, except for the angle $\angle O_bO_cH$ in the VDZ basis, where the error is 2−4%, the errors in the predicted geometrical attributes are ≪1% for all basis sets that are affordable to MRCI optimization. Indeed, there is no reason in principle why a similar performance cannot be anticipated for other (or larger) basis sets. In turn, the small differences observed in the geometric attributes corroborate the assumption (3) above, with such differences lying most likely within an optimistic value that may be expected for the accuracy of the calculations themselves. Because the calculations cover values of the active coordinate from 1.5 to 2.5 Å, there is also good reason to be confident in expecting a similar performance even outside such a range. Of course, a rigorous test at other distances would involve a considerable effort, which is unafordable for the title system but is currently being pursued for simpler prototypes. Note that the calculations headed by opt-CAS are much less expensive than the opt-

dx.doi.org/10.1021/ct200773b | J. Chem. TheoryComput. 2012, 8, 428−441

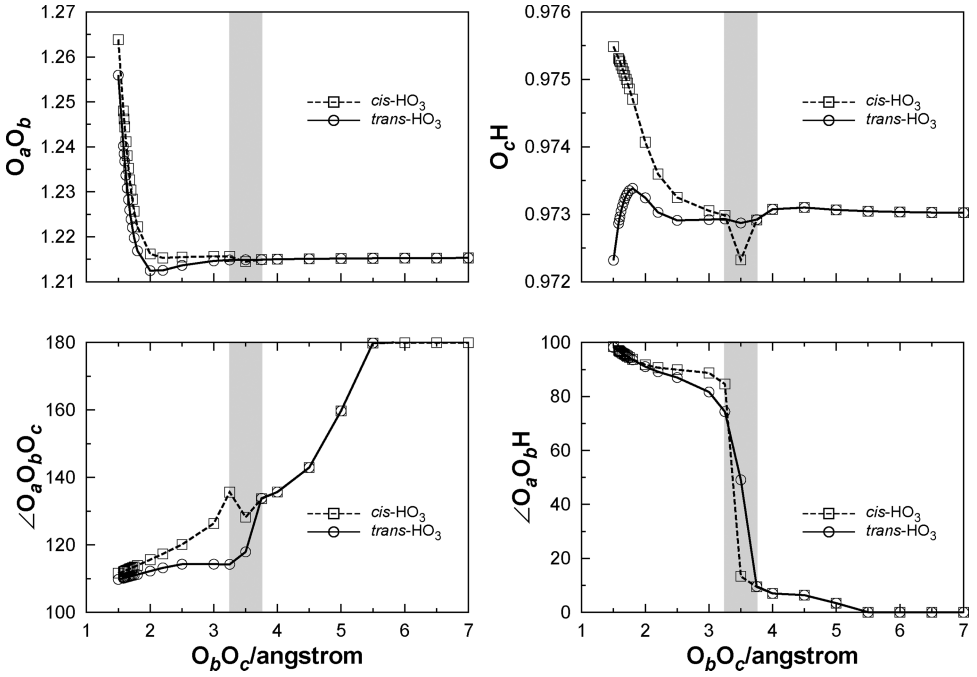

Figure 2. Variation of the nonactive coordinates in the coplanar reaction $HO_3 \rightarrow O_2 + OH$ along paths that cover both the equilibrium *cis*- and *trans*-HO_3 isomeric structures.

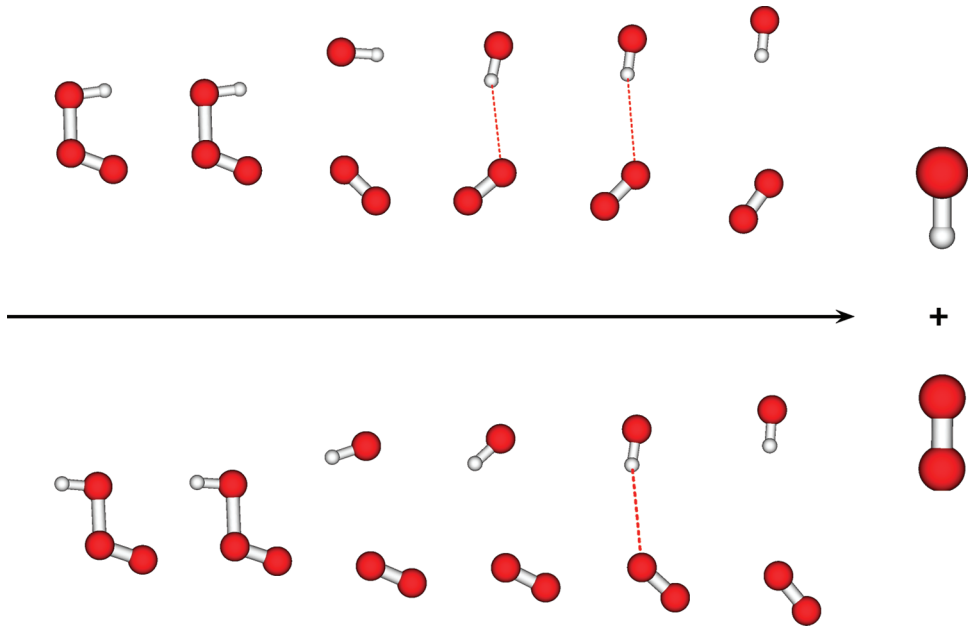

Figure 3. The reaction $HO_3 \rightarrow O_2 + OH$ as it progresses coplanarly in the sense indicated by the arrow and along paths chosen such as to encompass near the start either the *cis*- (top panel) or the *trans*-HO_3 (bottom) isomers (first and second structures in those panels). From left to right, the structures correspond to values of the active coordinate equal to 1.58, 1.68, 3.25, 3.50, 3.75, 4.50 and 5.50 Å. Note the fast variation in orientation over the transitional region where the binding character changes (see also Figure 2 and text).

MRCI ones, a difference that may surpass in orders of magnitude the time spent in MRCI+Q optimizations.

3.2.2. Major Topographical Features. We now turn to the energetics and detailed features of the optimum path for dissociation of HO_3 into O_2 + OH. Besides the curves reported elsewhere[12] with the VXZ ($X = T,Q$) basis set, results are now presented with both the optimized CAS path and single-point MRCI+Q calculations being carried out with the diffusely augmented AVXZ ($X = D, T, Q, 5$) basis (see later for $X = 6$). Here too, the raw energies have been subsequently CBS extrapolated pointwise by treating separately the CAS and dc energy contributions.[48,50] As before, the results corroborate our finding[12] that the Davidson correction plays a prominent role along the entire dissociation path.

Figure 2 illustrates the variation of the optimized coordinates for the predefined values of the inactive coordinate, with the drastic changes between 3.25 and 3.75 Å being clearly visible. At points inside this range, convergence is difficult with tight accuracy criteria, and hence the results (showing larger variations) should be viewed as approximate ones. The reasons

dx.doi.org/10.1021/ct200773b | J. Chem. TheoryComput. 2012, 8, 428–441

for this can be best understood from Figure 3 where snapshots of the various structures are shown as the inactive coordinate progresses toward dissociation (right-hand side of the panel). Clearly, the transition from the covalent-like $O_aO_bO_cH$ bonding (second panels from left-hand side) to the hydrogen-type bonding in $O_aO_b\cdots O_cH$ (central snapshots) is to be expected. Indeed, at even larger distances, the OH radical tends to align with O_2, as dictated by symmetry reasons[11] and shown in the right-most snapshots. At such distances, the permanent dipole−quadrupole electrostatic and induction forces are expected to be the dominant interactions (dispersion forces are not expected to arise or, at least, they should not play a significant role at the FVCAS level of theory).

Motivated by the possibility of finding stationary points in the above region of the PES, and given the long-range nature of the interactions dominating there, a few trial CAS/AVQZ calculations have been run. By allowing all degrees of freedom to optimize, a somewhat difficult to locate minimum has been predicted when a tight accuracy (a simultaneous gradient of <1 μE_h Å^{-1} and energy of <0.01 μE_h) was utilized. The corresponding structure and harmonic frequencies (denoted with a tilde to distinguish from those of the stable isomers) are shown in Figure 4. A full optimization yields a central OO bond

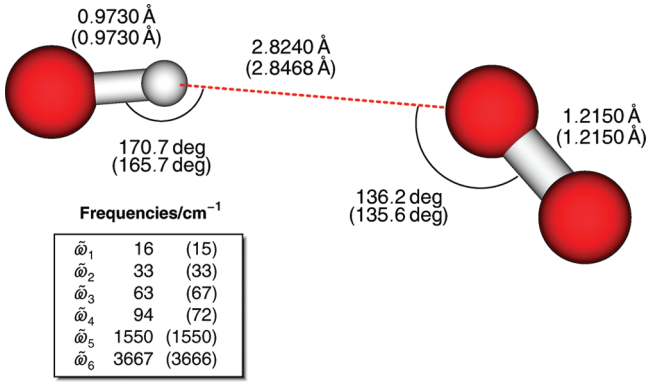

Figure 4. A planar van der Waals minimum of the OH···O_2 type as predicted (up to an energy of 10^{-5} E_h and gradient of 5×10^{-6} E_h Å^{-1}) at the CAS/AVQZ level of theory, thus virtually without taking into account any dispersion interaction, which is expected to arise only at the MRCI level. Results outside (inside) brakets are for a slightly nonplanar (planar) structure. The last quoted figure for bond lengths is likely to be uncertain.

distance of 3.86 Å, with a dihedral angle of −0.03°, which is shown in Figure 4. A constrained optimization preserving planarity has then been carried out, yielding a structure essentially identical to the latter (parameters in brackets). As for the "intermolecular" frequencies, two are low and two are somewhat larger (63 and 94 cm^{-1}, which correspond to out- and in-the-plane bending of OH, respectively). If the C_s geometry is assumed to be optimal, the above vdW structure is predicted to lie 0.138 kcal mol^{-1} (68 K) below the dissociation asymptote at the CAS/AVQZ level of theory and at 0.417 kcal mol^{-1} [0.345 kcal mol^{-1} = 174 K] when calculated with MRCI+Q/AVQZ [CBS(Q,5)/MRCI+Q]. The above does not imply that the true MRCI+Q minimum is planar, although all calculations here reported tend to suggest so. Note that another minimum related by symmetry is expected, as well as a saddle point connecting them, although no attempt is deemed to be justified here to enter into such an analysis.

The energetics of the dissociation process at the MRCI+Q/AV5Z//CAS/AVQZ level of theory are illustrated in Figure 5.

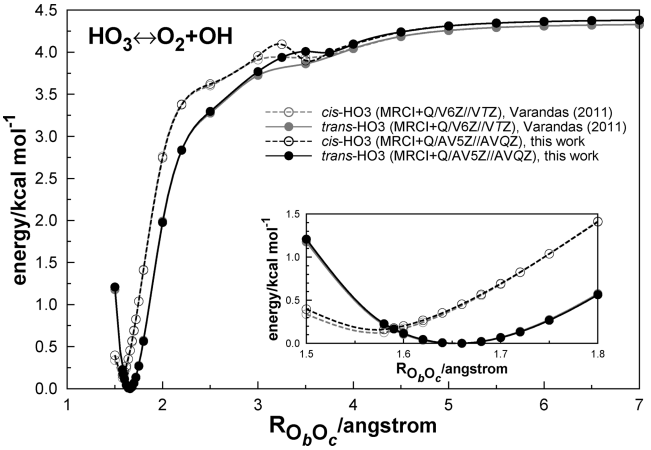

Figure 5. Raw MRCI+Q dissociation curves for the reaction $HO_3 \rightarrow O_2$ + OH as it progresses from the *cis*- and *trans*-HO_3 geometries (energies taken relative to the *trans*-HO_3 minimum).

Note that the paths shown encompass both the *cis*- and *trans*-HO_3 isomers, with the CBS results here reported allowing a direct comparison with the results presented elsewhere[12] but employing a V*X*Z basis. For this purpose, the previously reported MRCI/V6Z//CAS/V*T*Z results are also shown. Remarkably, and despite utilizing the lowest and one of the highest ranked correlation consistent basis sets, the results are seen to differ only slightly at long range, which may not be surprising due to the additional diffuse functions of the AV*X*Z basis set. Further confidence on the predicted general trends comes from the fact that the optimum CAS paths have themselves been obtained at distinct basis set levels, thus suggesting that the corresponding PESs are nearly parallel to each other. The corresponding results obtained via CBS extrapolation are illustrated in Figure 6. As shown in Figures 5

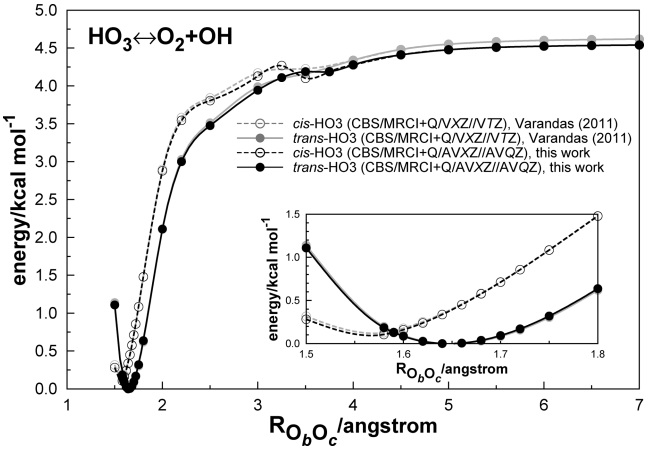

Figure 6. As in Figure 5 but for the CBS/MRCI+Q curves.[60]

and 6, no barrier is observed along the *cis*- and *trans*-HO_3 dissociation paths. Although one might anticipate their existence from Figure 8 in our previous work,[13] we recall that such a plot was meant to illustrate the use of a Fourier analysis as a means to obtain a full-dimensional PES from a rather limited amount of *ab initio* data, and hence extrapolations

dx.doi.org/10.1021/ct200773b | J. Chem. TheoryComput. 2012, 8, 428−441

Table 2. Predicted Geometries of *cis*- and *trans*-HO_3 Isomers at Various Levels of Theory[a]

	cis				*trans*				$\Delta E_{iso}^{x\,b}$	
X	O_bO_c	MRCI	O_bO_c	MRCI+Q	O_bO_c	MRCI	O_bO_c	MRCI+Q	MRCI	MRCI + Q
D	1.976	−0.561100	1.869	−0.604357	2.020	−0.561919	1.865	−0.605458	0.514	0.691
T	1.600	−0.725620	1.593	−0.782251	1.698	−0.726057	1.680	−0.782702	0.274	0.283
Q	1.579	−0.777365	1.576	−0.837629	1.683	−0.777725	1.664	−0.837984	0.226	0.223
5	1.572	−0.794311	1.568	−0.855565	1.672	−0.794563	1.655	−0.855812	0.158	0.155
6	1.569	−0.800139	1.566	−0.861730	1.670	−0.800367	1.653	−0.861950	0.143	0.138
(*T*,*Q*)	1.570	−0.808364	1.565	−0.871335	1.669	−0.808601	1.650	−0.871557	0.149	0.139
(*Q*,5)	1.568	−0.808323	1.564	−0.870583	1.665	−0.808485	1.647	−0.870736	0.102	0.096
(5,6)[c]	1.568	−0.807351	1.565	−0.869384	1.666	−0.807555	1.648	−0.869584	0.128	0.126

[a]Energies in hartree (after adding 225 E_h to the total energy), distances in angstroms, exothermicities of isomerization in kilocalories per mole. In this and the following table, the various sets of entries, starting at *D* and ending at the highest affordable pair of cardinal numbers used for the CBS extrapolation, refer only to MRCI/AV*X*Z//CAS/AV*Q*Z from this work. See Table 3 of the SI for other sets of results[12] also utilized in the analysis reported here. [b]The superscript *x* labels the method, MRCI or MRCI+Q. [c]Attributes interpolated from OO central bond distances of 1.50, 1.58, and 1.59 Å, for *cis*-HO_3; 1.62, 1.66, and 1.70 Å, for *trans*-HO_3.

should be viewed with caution (see also later). Interestingly, the classical dissociation energy at the CBS/MRCI+Q/V*X*Z//CAS/V*T*Z level of theory turns out now to be marginally larger than the CBS/MRCI+Q/AV*X*Z//CAS/AV*Q*Z one, whereas Figure 5 would lead one to expect an opposite trend. However, this may be understood by noting that the results obtained from calculations with a smaller basis are expected to predict a larger variation upon CBS extrapolation than the ones utilizing a more flexible basis set. Nevertheless, despite the reversal in order, the two CBS binding energies are predicted to differ only marginally from each other. This is best quantified from the numerical attributes of all calculated paths that are given in Tables 2 and 3 (for completeness, the entire set of results, including unreported numerical values referring to our previous work,[12] are given in Tables 3 and 4 of the SI). A statistical analysis of all CBS values suggests a classical dissociation energy of $4.6_5 \pm 0.1$ kcal mol^{-1}, where the subindex indicates the first uncertain digit. A similar analysis for the *cis*-HO_3 isomer yields a slightly lower value of $4.5_1 \pm 0.1$ kcal mol^{-1}. Given that both isomers dissociate to the same asymptote, can such a slightly lower stability be able to explain by itself the failure of the FTMW work to see clear evidence of the latter? Although an answer cannot be given prior to a full-dimensional analysis of the dynamics, the present results suggest that an easier route for dissociation of HO_3 to take place is at least potentially available.

Table 3. Predicted Classical Dissociation Energy[a] for the *cis*- and *trans*-HO_3 Isomers at Various Levels of Theory

	cis		*trans*	
X	MRCI	MRCI+Q	MRCI	MRCI+Q
D	0.632	1.492	1.146	2.183
T	2.103	3.574	2.377	3.857
Q	2.440	4.056	2.665	4.279
5	2.579	4.238	2.737	4.393
6	2.648	4.321	2.791	4.460
(*T*,*Q*)	2.802	4.530	2.951	4.669
(*Q*,5)	2.753	4.455	2.855	4.551
(5,6)	2.740	4.431	2.868	4.556

[a]In kilocalories per mole. See also Table 2 and Table 4 of the SI.

3.2.3. The cis- and trans-HO_3 Isomers. A first observation concerns the optimum geometries (location of the minima), especially in what concerns the central OO bond distance, which tends to differ slightly from the value commonly judged as "experimental". Specifically, for the *trans*-HO_3 isomer, the best estimates for the O_bO_c bond length fall close to 1.65 Å with a realistic average and very conservative error margin [cf. *Q*Z values in Table 1 of the SI and Table 2, which suggest 1.650 ± 0.002 Å] being 1.66 ± 0.01Å, thus somewhat shorter than the commonly accepted value of 1.688 Å but significantly larger than predicted (≤1.61 Å) from single-reference CCSD(T) calculations. Recall that the "experimental" value has been obtained[17] from rotational transitions of HO_3 and DO_3 assuming the O_aO_b and O_cH bonds fixed at the equilibrium MRCI values (with which we perfectly agree at the MRCI/V*Q*Z level of theory; Table 1 of the SI and Table 2). Constraints have therefore been imposed, which can be in error. Similarly, the exothermicity for isomerization shown in Table 2 is seen to consistently converge to our own MRCI+Q prediction[13] of $\Delta E_{iso} = 0.12 \pm 0.05$ kcal mol^{-1}, only slightly smaller than the value of 70 cm^{-1} = 0.20 kcal mol^{-1} inferred from experiment results. Indeed, an average of all tabulated CBS/MRCI+Q extrapolated values yields 0.13 kcal mol^{-1}, in excellent agreement with our previous[13] estimate.

In a second observation, we address the question: what are the best structural parameters for the *cis*- and *trans*-HO_3 isomers at the CBS level of theory? Rather than extracting such data from a very expensive grid of CBS points, the premise presented earlier is once more invoked to suggest that the result can be well approximated by fixing the O_bO_c bond distance at the minimum obtained at a given CBS/MRCI+Q level with the HO_3 geometry being optimized at the CAS level with the best basis set available of the correct kind. The results so obtained are reported in Table 4 (and Table 2 of the SI) for the V*X*Z and AV*X*Z basis by carrying out CAS/V6Z and CAS/AV6Z optimizations at the O_bO_c distances obtained from the CBS(5,6)/MRCI+Q/V*X*Z and CBS(*Q*,5)/MRCI+Q/AV*X*Z calculations. Naturally, there may be a slight difference due to having employed a finite cardinal number for the optimizations, but the error is within the accuracy expected for such attributes. Indeed, the geometries in Table 4 (predicted up to 1 μE_h Å^{-1}) show a remarkable consistency (within a few thousandths of an Ångstrom, and few hundredths of a degree) irrespective of basis set. Refined parameters could be obtained self-consistently by performing MRCI+Q calculations on structures close to and bracketing the minimum and repeating the procedure until the interpolated central OO bond distance is converged to the same value in both calculations. This has not been deemed necessary. Of course, if the focus is on forces rather than

Table 4. Optimum *cis* and *trans* Structures of HO_3 at the CBS/VXZ and CBS/AVXZ Levels of Theory As Determined from the Scheme Devised in the Present Work[a]

method/basis	R_{OaOb}	R_{ObOc}	α	R_{OcH}	β	ϕ
			cis			
EOMIP-CCSD/ANOI[b]	1.24	1.57	112.24	0.97	96.96	0.0
CBS/VXZ[c]	1.2505	1.5658	111.97	0.9751	97.29	0.0
CBS/AVXZ[d]	1.2508	1.5637	111.96	0.9751	97.33	0.0
			trans			
EOMIP-CCSD/ANOI[b]	1.23	1.61	111.71	0.97	96.73	180.0
CBS/VXZ[c]	1.2293	1.6497	110.49	0.9729	95.79	180.0
CBS/AVXZ[d]	1.2296	1.6473	110.48	0.9729	95.83	180.0
exptl.[e]	1.225	1.688	111.0	0.972	90.0	180.0

[a]Distances in angstroms, angles in degrees. See elsewhere[13] for further comparisons and references to other work, and Table 2 of the SI for the associated vibrational frequencies. [b]From equation-of-motion coupled-cluster-for-ionized-states calculations[14] with the triple-ζ contraction of the atomic natural orbitals basis set of Almlöf and Taylor.[61] [c]Obtained from the CAS/V6Z optimization with the O_bO_c bond length kept innactive and fixed at the optimum value determined by interpolation from CBS(5,6)/MRCI+Q/VXZ//CAS/VQZ calculations. [d]Obtained from the CAS/AV6Z optimization with the O_bO_c bond length kept innactive and fixed at an optimum value determined by interpolation from CBS(Q,5)/MRCI+Q/AVXZ//CAS/AVQZ calculations. [e]From Suma et al.[17]

geometrical parameters, then the calculation of a CBS grid of points may be mandatory. Interestingly, our results show an enhanced agreement with the calculations[14] carried out using the equation-of-motion coupled-cluster-for-ionized-states (EOMIP-CCSD*) method and the triple-ζ contraction of the atomic natural orbitals basis set of Almlöf and Taylor.[61] In fact, they essentially overlap within the accuracy reported for the EOMIP-CCSD* results in *cis*-HO_3, while the difference in the central OO bond distance of the *trans* isomer is reduced to 0.04 Å or so. This may not be totally surprising as EOMIP-CCSD is believed (when used judiciously) to allow[14] for treatment of the nondynamical correlation associated with the multireference character. On the other hand, besides falling short by about 0.04 Å relative to the commonly accepted "experimental" value of the O_bO_c bond distance, our results predict an angle $\angle O_bO_cH$ of ~96°, in agreement with all directly optimized MRCI estimates but nearly ~6° larger than the "experimental" value.[17] One may think of going a step further and calculating the harmonic frequencies at such optimized geometries. Naturally, only by accident would the gradient norm vanish at a geometry so determined, since this would imply a true stationary point. In fact, it is small but nonzero (typically $\lesssim$0.015 a.u.) due to the dislocation along the central OO bond distance, which has been optimized by interpolation from the CBS/MRCI+Q calculations. However, this does not imply that the calculated harmonic frequencies have themselves no meaning. Indeed, Table 2 of the SI shows that the method yields values in good agreement with the best available estimates, including for the fundamental associated with the stretching of the central OO bond which tends to lie closer to the observed fundamentals. It therefore remains to be seen whether a new simulation that takes into account the structural parameters here reported (eventually by allowing for their variation with torsion angle[13]) can mimic the observed[17] HO_3 and DO_3 rotational spectra.

3.2.4. Bond-Breaking Energy and Onset of Hydrogen Bonding. We now turn to the analysis of the small bump that appears in the range where the central OO bond breaks to form a hydrogen-type one. This is best seen from Figures 7 and 8,

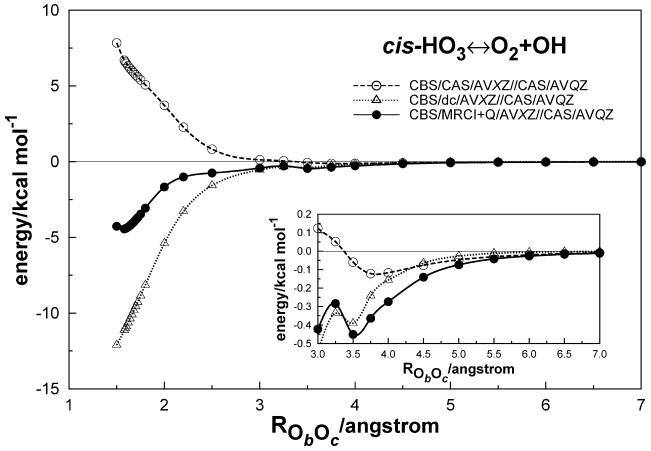

Figure 7. CBS extrapolated CAS and dynamical correlation components of the energy along the path for the reaction *cis*-HO_3 → O_2 + OH (energies taken relative to the asymptote).

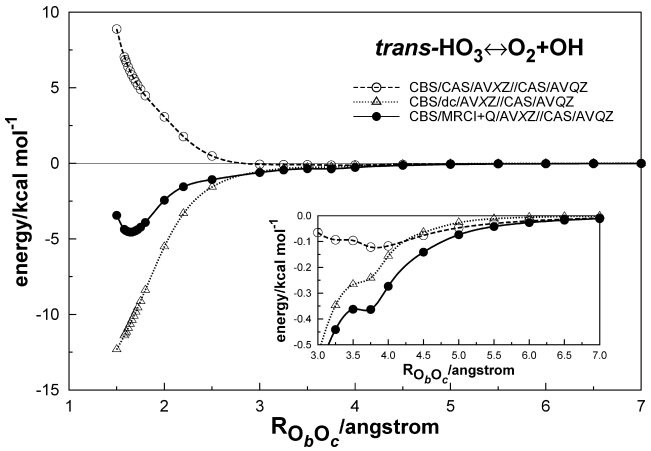

Figure 8. As in Figure 7 but for the reaction *trans*-HO_3 → O_2 + OH.

which show the variation of the CAS and dynamical correlation components of the energy along the paths involving the *cis*-HO_3 and *trans*-HO_3 isomers, respectively. The notable feature from both of these plots is that the CAS energy is repulsive in nature with only a shallow minimum arising at a central OO distance of 3.8 Å or so, which is likely due to electrostatic and induction type attractive forces between the O_2 and OH fragments. In fact, such interactions are the ones to be expected at the FVCAS level of theory since the dispersion energy involves single excitations from both fragments into the virtual space that are only considered at the CI level. As the bond stretches beyond the equilibrium distance of this shallow minimum, the energy raises toward the dissociation asymptote. It turns out that the dynamical correlation energy itself shows a small plateau (apparently a well for the *cis* structure) near the minimum at the FVCAS level of theory, which goes on to yield a deeper van der Waals well at MRCI+Q level of theory. Clearly, if there is such a minimum, a saddle point must arise

dx.doi.org/10.1021/ct200773b | J. Chem. TheoryComput. 2012, 8, 428–441

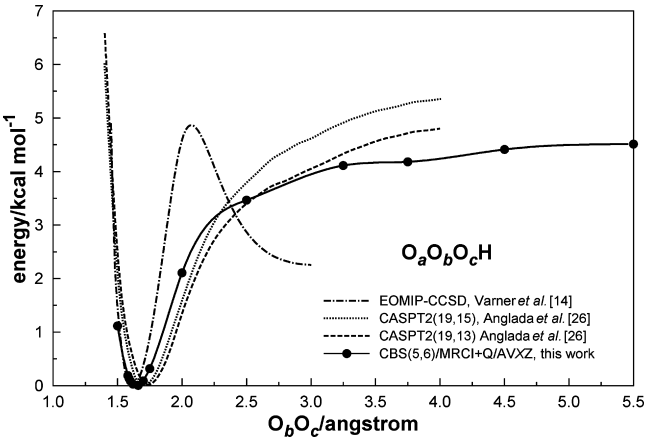

Figure 9. A comparison of recently calculated curves[20,33] for dissociation of *trans*-HO_3 with the CBS(5,6)/MRCI+Q/AV*X*Z//CAS/AVQZ curve to be discussed later in this work (energies taken relative to the minimum).

connecting it to the *cis* and *trans* chemical minima of HO_3. One may then view this as a reminiscence that marks the end of covalent bonding and onset of a van der Waals (vdW) type interaction. In fact, such a scar signaling the transition between the two distinct involved bonding types arises more frequently than probably anticipated. Note that the minimum energy path for the rupture of a chemical bond should reflect the bond directionality, which is not necessarily coincidental with the preferred one to yield maximum stability to the vdW species that is subsequently formed. This is particularly so when the dominant forces are of the electrostatic type, such as in hydrogen bonding, where the directionality is mostly defined by the preferred orientation of the leading permanent electrostatic moments (in this case, the dipole of OH and quadrupole of O_2). A more prominent example is possibly provided by hydrogen peroxide. In this case, such a manifestation of distinct directionalities can be even more severe upon rupture of the central OO bond, since each OH fragment has a permanent dipole moment.[62,63] Similar features can also be observed in the PES for the electronic ground state of HO_2, as predicted long ago[64] and more recently corroborated by accurate *ab initio* studies.[65] Still another example where bond rupture yields an atom plus a diatom is the ground state of O_3, which shows[66] a weak O···O_2 van der Waals well separated by a tiny barrier from the deep well associated with the chemically stable ozone molecule; the van der Waals (vdW) attraction should now be due mostly to electrostatic (quadrupole−quadrupole) and dispersion forces involving O(^3P) and O_2. Note that in the two last cases, the atomic quadrupole should be the one to reorient since this involves only electronic motion, a faster process than when nuclei are involved, as suggested long ago when developing the so-called relaxed quadrupole moment model.[67,68] Of course, one should be cautious by recalling that minima often arise due to avoided intersections, although as discussed later, this does not appear to be the case here. In fact, for the latter, the barrier is expected to lie above dissociation[69] as opposed to the cases here examined where it is positioned below the asymptote. Thus, this may be the unique feature that characterizes the situations reported above. Of course, the analysis presupposes an accurate treatment since poor basis sets or methodologies may undermine the true picture.[69] In this regard, we note that the appearance of the above minimum is not clear from the recently reported[33] CASPT2 curves, although a slight tendency to develop a kink is apparent at a somewhat shorter distance of ∼3 Å, particularly along the CASPT2(13,11)/AVTZ profile. Note that this curve has a behavior similar to ours with a just slightly higher dissociation limit, while the CASPT2(19,15)/AVTZ curve[33] suggests an asymptote even higher by about 0.5 kcal mol^{-1}. Unfortunately, despite the excellent agreement achieved in this case for D_0 [= 3.0 kcal mol^{-1}, when the ZPE correction is determined from the CAS(19,15)/AVTZ harmonic vibrational frequencies], it is hard to tell how the method behaves upon the choice of other active spaces or how convergence is enhanced with increase of basis set toward the CBS limit. Interestingly, the EOMIP-CCSD* curve reported by Varner et al.[20] also predicts its highest energy point to be nearly 5 kcal mol^{-1} above the *trans* minimum. However, rather than flattening, their curve drops markedly after this point to reach the asymptote at 2.5 kcal mol^{-1} or so above the bottom of the well. Note that the existence of such a significant barrier conflicts with experimental evidence that shows a strong negative temperature-dependence for the association reaction[10,22] OH + O_2 → HO_3, a result that is considered to be typical of a barrier-free reaction. Of course, the barrier which seems to develop on the PES reported in Figure 8 of our previous work[13] should not be surprising, since it stems from CBS/CCSD(T) calculations.

As noted above, the appearance of a very shallow minimum and a tiny barrier at mid distances, as in the cases here reported, may raise the possibility of them being due to an avoided intersection. With this in mind, three-state CAS/AV5Z//CAS/AVQZ calculations have been carried out for the title system. The results for the *trans*-HO_3 isomer are shown in Figure 10.

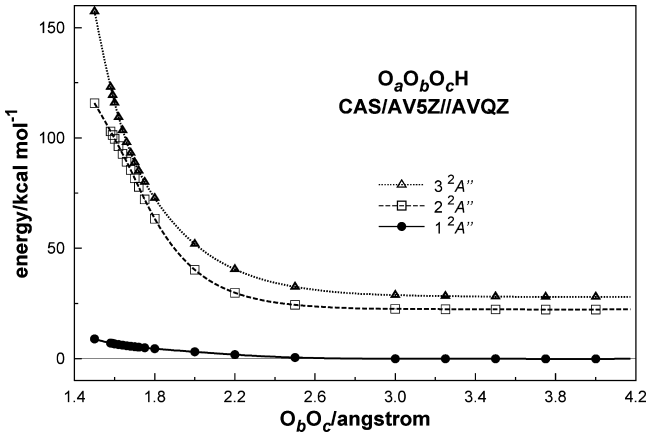

Figure 10. The first three electronic states of $HO_3(^2A'')$ along the dissociation curve of the *trans* isomer at the CAS/AV5Z level of theory (energies taken relative to the lowest asymptote: ground-state products).

Clearly, the first and second excited state curves lie high up in energy relative to the ground state (and the lowest excited state of $^2A'$ symmetry[11]), with the dissociation yielding[70−72] OH($X^2\Pi$) and O_2 in the $a^1\Delta_g$ and $b^1\Sigma_g^+$ states. Thus, there is no evidence of an avoided intersection involving the ground state curve at the region of interest (there appears to be one at short distances but between the first two $^2A''$ excited states). A similar conclusion stems from the dissociation path that starts at *cis*-HO_3 (hardly distinguishable from *trans*-HO_3), which is omitted for brevity. No changes that may alter this scenario are expected if the "physical" dynamical correlation is included.

dx.doi.org/10.1021/ct200773b | J. Chem. TheoryComput. 2012, 8, 428−441

3.2.5. Zero-Point Energy Corrected Dissociation Energy. Because the saddle points referred to above are expected to lie below the dissociation asymptote, they should have no drastic implications on the kinetics of the association/dissociation reaction. Indeed, even if they may manifest as resonance states, no such evidence has been reported. Consider then the dissociation energy (D_0) for the reaction $O_2 + OH \rightleftharpoons HO_3$. Assuming as usual the *trans* isomer, the ZPE correction[10,14,20] will be defined as the difference between the ZPE of *trans*-HO_3 and the sum of the ZPE values of O_2 and OH (asymptote), yielding $D_0 = D_e - \Delta E^{as}_{ZPE}$, where "as" stands for asymptote. Using experimental data,[70] one obtains $E^{as}_{ZPE} = 2659$ cm^{-1}, a value that compares accurately with the results obtained from force calculations at the MRCI/AVQZ level of theory,[73] 2662 cm^{-1}. Following Varner et al.,[20] we now define the ZPE of *trans*-HO_3 from the fundamentals inferred from the combination bands observed by Lester and co-workers.[25] Unfortunately, only five frequencies could be spectroscopically observed, possibly because the one corresponding to the terminal OO stretch had a weak oscillator strength. Using the average value of the fundamentals of OH stretch (ν_1) and ν_3 to ν_6 determined from their combination bands plus the theoretical harmonic frequency[20] of $\omega_2 = 1331$ cm^{-1}, one obtains $ZPE_{t\text{-}HO_3} = 3352$ cm^{-1}. The ZPE correction will therefore be $\Delta E^{as}_{ZPE} = 1.98$ kcal mol^{-1}. By subtracting this value from the classical dissociation energy of $4.6_5 \pm 0.1$ kcal mol^{-1} here predicted (as determined from all CBS extrapolated binding energies in column 5 of Table 3), the dissociation energy assumes a value of $D_0 = 2.6_7 \pm 0.1$ kcal mol^{-1}. Two observations are in order at this point. First, our value of ΔE^{as}_{ZPE} is somewhat smaller than 2.33 kcal mol^{-1}, the estimate reported by Varner et al.,[20] which is possibly due to the different data used for the diatomics. Second, one may consider replacing their value of 1331 cm^{-1} utilized for the O_aO_b fundamental (only ~32 cm^{-1} smaller than our own CBS/VXZ value in Table 2 of the SI) with the one predicted at the MRCI level of theory,[13] 1421 cm^{-1}. If done, a ZPE correction relative to the asymptote of[73] $\Delta E^{as}_{ZPE} = 2.11$ kcal mol^{-1} is obtained, yielding $D_0 = 2.5_4 \pm 0.1$ kcal mol^{-1}. Both values agree well with our earlier result,[12] although it is difficult to comment on their relative accuracy since our MRCI fundamental utilizes a modest VTZ basis. However, the difference may help on setting a fairly conservative uncertainty to read $D_0 = 2.6_7 \pm 0.1$ kcal mol^{-1}. Having gone this far, one may also think of utilizing the highly reliable set of CAS-type vibrational frequencies labeled CBS/VXZ in Table 2 of the SI. However, since experimental data are available for five such fundamental frequencies, the above harmonic frequencies obtained from the CAS calculations may be scaled to improve agreement with experimenta results, particularly keeping in mind that they only account for static correlation and ignore core (as well as other small/minor) effects, besides anharmonic effects. As shown in Figure 11 and Table 5, a linear fit (with an intercept at the origin of -26 ± 6 cm^{-1}: fit I) yields a respectable scaling factor of 0.96, which compares with values[74] of ~0.9 for HF and 0.97 for MP2 calculations. Note that the experimental frequencies[25] have been labeled differently from here where they have simply been ordered by increasing value, and hence the notation $\tilde{\nu}_i$ is employed instead. The above procedure leads to $ZPE_{t\text{-}HO_3} = 3345$ cm^{-1} and a ZPE correction of $\Delta E^{as}_{ZPE} = 1.95$ kcal mol^{-1}, from which a value of $D_0 = 2.7_0$ kcal mol^{-1} follows in close agreement with the value predicted above. A slightly smaller value of $ZPE_{t\text{-}HO_3} = 3313$ cm^{-1} is obtained if the CCSD(T) and MRCI(Q) force calculations[13] (with basis sets of highest affordable cardinal number) are included. From this fit II, with an abcissa at the origin of -2 ± 1 cm^{-1}, one gets $D_0 = 2.8_0$ kcal mol^{-1}. Thus, $D_0 = 2.7 \pm 0.2$ kcal mol^{-1} will provide a realistic estimate with a very conservative error bar in order to embrace our previous estimate[12] and partly reflect the still substantial uncertainty in the ZPE, while a more focalized value from this work is $D_0 = 2.8 \pm 0.1$ kcal mol^{-1}.

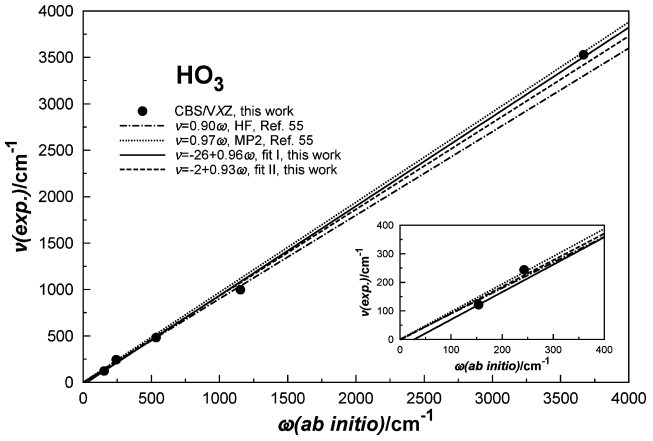

Figure 11. Calculated versus experimental vibrational frequencies for the *trans*-HO_3 isomer.

3.2.6. Use of Even Larger Basis and Role of Davidson's Correction. Before concluding, we address two complementary quests. The first refers to the HO_3 dissociative pathways by carrying further MRCI and MRCI+Q/AV6Z//CAS/AVQZ calculations, as well as CBS(5,6)/MRCI+Q extrapolations. Due to being rather expensive, they have been done at every other point. Shown in Tables 2 and 3, the results corroborate those reported above while stressing that CBS extrapolation can attain a sort of accuracy only achievable by raw calculations using basis sets with cardinal numbers at least two units larger. Indeed, a CBS(T,Q) extrapolation seems to be all one requires if an accuracy of 0.1 kcal mol^{-1} is sought, with CBS(Q,5) attaining already the realm of hundredths of kcal mol^{-1}. Indeed, a CBS(5,6)/MRCI+Q estimate of the well depth of the vdW structure in Figure 4 yields a value of 0.355 kcal mol^{-1} = 179 K, thus within a few K of the earlier reported one. If the energy at 100 Å is instead used as the dissociation limit, the CBS(5,6)/MRCI+Q [CBS(5,6)/MRCI] result is 180 K [157 K], thus corroborating our above analysis of this issue. No attempt to optimize the midrange (prereactive) stationary points of HO_3 at the MRCI level of theory has been made due to being unaffordable. A wider characterization of the vdW region of the PES must await calculation of a multidimensional grid of points with a view to improve the existing global PES,[30] a topic that is outside the scope of this work. Recall that an optimization and force calculation may take months of uninterrupted work on a double-core double-processor, even for the cheapest basis here utilized, rather than <1 day per grid point optimized at the CAS/AVQZ level followed by a single-point MRCI/AV5Z//CAS/AVQZ calculation.

The other quest centers on Davidson's correction, whose inclusion in the MRCI expansion has been shown to be of key importance. Strictly speaking, the (+Q) correction ignores the contribution due to triple excitations and approximately corrects for quadruple excitations.[75] Indeed, it usually overestimates the contribution due to quadruple excitations, being

Table 5. Experimental vs Predicted Vibrational Frequencies[a] of *trans*-HO_3

		calcd		fit I[b]		fit II[c]		
frequency	exptl[d]	MRCI[e]	CBS/VXZ[f]	value	error[g]	value	error[g]	assignment
$\tilde{\nu}_1$	122 ± 7	147.61	154.01	121.69	0	141.61	16	torsion
$\tilde{\nu}_2$	244	222.04	243.00	207.33	−15	224.62	−8	central OO stretch
$\tilde{\nu}_3$	482	501.41	535.23	488.57	1	497.22	3	OOO bend
$\tilde{\nu}_4$	998	1094.27	1153.50	1083.62	8	1074.01	8	HOO bend
$\tilde{\nu}_5$		1421.35	1363.50	1285.68		1269.87	−3	terminal OO stretch
$\tilde{\nu}_6$	3528	3761.91	3668.37	3503.86	−1	3419.94		OH stretch
ZPE		3574.30	3558.80	3345.38		3313.63		
ZPE[h]		10.219	10.175	9.565	5	9.474	8	

[a]Unless indicated otherwise, all values are in inverse centimeters. [b]From the fit $\tilde{\nu}_{exp} = (-26 \pm 6) + (0.96 \pm 0.02)\omega_{calc}$. The CBS/AVXZ results differ very little from those here reported and hence are not given. [c]From a fit similar to *b* but including the values from force calculations[13] at the CCSD(T) and MRCI(Q) levels of theory with the basis sets of highest affordable cardinal number: $\tilde{\nu}_{exp} = (-2 \pm 1) + (0.93 \pm 0.01)\omega_{calc}$. A weight 10 times larger was then given to the corresponding lowest MRCI(Q)/VTZ frequency. [d]Data extracted from Table 1 of Derro et al.[25] See also the text. [e]Harmonic frequencies ω_i from MRCI/VTZ force calculations.[13] [f]Harmonic frequencies ω_i from this work CAS/V6Z force calculations at a geometry where all coordinates have been optimized but the value of the optimum central OO bond distance which was determined by interpolation from CBS(5,6)/MRCI+Q/VXZ//CAS/VQZ calculations at fixed O_bO_c bond lengths. All values have been assigned an equal least-squares weight but for the smallest frequency associated with torsion which has received a weight 10 times larger. See also Table 2 of the SI and the text. [g]Calculated − observed errors in %. [h]Energies are in kcal mol^{-1}. Under the error heading is given the average unsigned error (in %).

loosely often looked at as correcting for excitations beyond singles and doubles. Thus, it can help in improving size-consistency, which is expected to be critical in defining the proper dissociation asymptote. On the other hand, the dramatic role here played may also be a warning to signal unreliability. This led us to perform a test that may unravel potential difficulties. Although the natural choice would be to perform some test FCI calculation, this could only tell whether the MRCI+Q energy would be close to its exact absolute value. Thus, little could be gathered with respect to the relative energy since the BSSE would likely not have the same effect in both cases. Moreover, a FCI calculation would require a minimum amount of 6.6 EB = 1.8×10^{18} B = 6.6×10^9 GB, an out of step requirement. A simpler test consists of fitting the dynamical correlation to a damped dispersion form of the type $C_6\chi_6(R_{O_bO_c})R^{-6}$, where $\chi_6(R_{O_bO_c}/\rho)$ is a charge-overlap damping function[76] embedding a scaling parameter (ρ) to mimic the charge-overlap onset, and C_6 is an effective induced dipole-induced dipole dispersion coefficient. By treating C_6 and ρ as adjustable parameters, a satisfactory fit is obtained over the entire range of central OO bond distances, with the results for the *trans*-HO_3 path being of $C_6 \sim 25$ E_h a_0^6 and $C_6 \sim 28$ E_h a_0^6 at the MRCI and MRCI+Q levels of theory (in both cases, a value of $\rho \sim 5.7$ Å is obtained). Although no rigorous estimate of the leading dispersion coefficient for the title system is to our knowledge available for comparison, the above values fall close to the spherically averaged estimate of[77,78] $C_6 \sim 24$ or[79] 28 E_h a_0^6 for the F−O_2 isoelectronic interaction (values obtained from the geometric mean of C_6 for the F−F and O_2−O_2 homonuclear interactions). Because the above values differ only moderately (∼11%) from each other, this may provide compelling evidence to support the reliability of the results here reported at both levels of MRCI theory. Obviously, a firm conclusion on the validity of the +Q correction can hardly be expressed prior to a FCI calculation which, as noted above, is an impossible task at present for the title system, particularly with a basis of the correlation consistent type.

4. SUMMARY OUTLINE

A cost-effective scheme has been suggested to carry out *ab initio* calculations of PESs along bond-breaking/forming reaction paths at a level of accuracy that would be unaffordable otherwise. State-of-the-art MRCI+Q calculations using large correlation consistent basis sets of the Dunning type illustrated the method for the dissociation of HO_3, with the raw energies subsequently extrapolated to the CBS limit. The torsional potential of HO_3 has also been revisited.[13] Interestingly, the dissociation is predicted to occur in the plane of the molecule both for the *cis*- and *trans*-HO_3 isomers. As a result, the minimum of the calculated dissociation profiles is located at the equilibrium value of the central OO bond distance. This allowed us to extract a wealth of information on the optimum O_bO_c distance, which had so far been seldom reported. Of course, the accuracy so obtained when compared with full optimization at the MRCI level depends on the realism of the four-point premise here advanced, which has been shown to be good. The new results suggest that the value commonly accepted for the O_bO_c distance and taken as "experimental" is likely overestimated, although the new estimate is considerably larger than the values predicted from single-reference correlated calculations. Because this distance is known to play a critical role in the analysis of the rovibrational spectroscopic data of HO_3, the experimental data should desirably be reanalyzed by taking into account the novel information here reported.

Recently,[12] we advanced a few reasons to explain a small discrepancy between our best results and those inferred from the CRESU experiments: first and foremost, the unknown and much discussed effect in D_0 of anharmonicity,[14] and/or contributions from quasi-bound states above the dissociation limit.[40,41] Although the disagreement has been further reduced here by reanalizing the calculated vibrational frequencies against the known spectroscopic values, the above issue still awaits a definite answer. Other invoked reasons were of pure computational origin. First, we had adhered for affordability[12] to small correlation consistent basis. This has been overcome in the present work by using diffusely augmented basis functions both for the optimization of the CAS path and for the subsequent single-point MRCI calculations. Second, motivated by the key role played by Davidson's correction, doubts were cast on whether even higher multiple electronic excitations could make a difference. Clearly, an answer to this issue requires a FCI treatment, a task hardly foreseeable at present. Core effects and

relativistic corrections have been ignored; however, on the basis of the arguments presented earlier in the text, this should not significantly affect the dissociation energy (as can be seen from the errors on the vibrational frequencies[74]). The discrepancy then observed[12] between the average experimental value of the dissociation energy (D_0) and the corresponding theoretical prediction, which is here significantly mitigated, should then be viewed as minor and expectable for two basic reasons: first, because the theoretical method must unavoidably be approximate, both in principle and practice, as is here the case (recall the four-point premise); second, because HO_3 poses nontrivial problems to experimentation, as shown by the diversity of D_0 estimates [varying in recent years from the upper limit of[24] 6.12 kcal mol^{-1} and subsequently[21] 5.31 kcal mol^{-1} to the most recent and accurate value[14,22] of 2.9 ± 0.1 kcal mol^{-1}]. Indeed, the smaller value of D_0 now accepted as most accurate drastically changed our perspective on the role of the reaction of association of OH radicals with O_2, which passed from being considered as important[20,21] to having no meaning in the chemistry of Earth's atmosphere.[10,14,22] Meanwhile, the calculations reported elsewhere[12,13] and the ones presented here have shown the best consistent agreement thus far obtained with the experimental results[14,21,22] for both attributes (isomerization and dissociation) of the HO_3 radical. In particular, the current prediction for D_0 seems to support and even slightly enhance the finding[10,14,22] that HO_3 is likely to play a minor role in atmospheric chemistry; i.e., its fractional concentration $[HO_3]/([HO_3] + [OH])$ may turn out to be even slightly smaller than recently predicted,[10,14,22] thus only a few per thousand at all altitudes in the Earth's atmosphere. Of course, accurate kinetic calculations on a full-dimensional PES will be required to obtain improved theoretical estimates. Further work on the title system, as well as applications to other systems that might validate the generality of the scheme here suggested (in particular when more than one coordinate is required to become inactive), would therefore be valuable and most welcome.

■ ASSOCIATED CONTENT

Supporting Information

The complete set of relevant *ab initio* energies and structural parameters. This information is available free of charge via the Internet at http://pubs.acs.org/.

■ AUTHOR INFORMATION

Corresponding Author

*E-mail: varandas@qtvs1.qui.uc.pt.

Notes

The authors declare no competing financial interest.

■ ACKNOWLEDGMENTS

This work has the support of Fundação para a Ciência e a Tecnologia (contracts PTDC/QUI-QUI/099744/2008 and PTDC/AAC-AMB/099737/2008), Portugal.

■ REFERENCES

(1) Paldus, J. In *Theoretical Chemistry: Advances and Perspectives*; Eyring, H., Henderson, D., Eds.; Academic Press: New York, 1976; Vol. 2, p 131.
(2) Sherrill, C. D.; Schaefer, H. F. III. *J. Phys. Chem.* **1996**, *100*, 6069.
(3) Khait, Y. G.; Song, H.; Hoffmann, M. R. *Chem. Phys. Lett.* **2003**, *372*, 674.
(4) Khait, Y. G.; Jiang, W.; Hoffmann, M. R. *Chem. Phys. Lett.* **2010**, *493*, 1.
(5) Bytautas, L.; Ruedenberg, K. *J. Chem. Phys.* **2004**, *121*, 10905.
(6) Szalay, P. G.; Muller, T.; Gidofalvi, G.; Lishka, H.; Shepard, R. *Chem. Rev.* In press. DOI: dx.doi.org/10.1021/cr200137a.
(7) Langhoff, S. R.; Davidson, E. R. *Int. J. Quantum Chem.* **1974**, *8*, 61.
(8) Werner, H.-J.et al. MOLPRO, version 2008.3, a package of *ab initio* programs. http://www.molpro.net (accessed Jan 2012).
(9) Knowles, P. J.; Schütz, M.; Werner, H. In *Theoretical Chemistry: Advances and Perspectives*; Grotendorst, J., Ed.; John von Neumann Institute for Computing: Jülich, Germany, 2000; Vol. 3; pp 97.
(10) Smith, I. W. M.; Picard, S. D. L.; Tizniti, M.; Canosa, A.; Sims, I. R. *Z. Phys. Chem.* **2010**, *224*, 949.
(11) Yang, J.; Li, Q. S.; Zhang, S. *Phys. Chem. Chem. Phys.* **2006**, *9*, 466.
(12) Varandas, A. J. C. *Phys. Chem. Chem. Phys.* **2011**, *13*, 15619.
(13) Varandas, A. J. C. *Phys. Chem. Chem. Phys.* **2011**, *13*, 9796.
(14) Beames, J. M.; Lester, M. I.; Murray, C.; Varner, M. E.; Stanton, J. F. *J. Chem. Phys.* **2011**, *134*, 044304.
(15) Cacace, F.; de Petris, G.; Pepi, F.; Troiani, A. *Science* **1999**, *285*, 81.
(16) Nelander, B.; Engdahl, A.; Svensson, T. *Chem. Phys. Lett.* **2000**, *332*, 403.
(17) Suma, K.; Sumiyoshi, Y.; Endo, Y. *Science* **2005**, *308*, 1885.
(18) Dunning, T. H. Jr. *J. Chem. Phys.* **1989**, *90*, 1007.
(19) Mansergas, A.; Anglada, J. M. *Phys. Chem. Chem. Phys.* **2007**, *9*, 5865.
(20) Varner, M. E.; Harding, M. E.; Vázquez, J.; Gauss, J.; Stanton, J. F. *J. Phys. Chem. A* **2009**, *113*, 11238.
(21) Murray, C.; Derro, E. L.; Sechler, T. D.; Lester, M. I. *Acc. Chem. Res.* **2009**, *212*, 419.
(22) Le Picard, S. D.; Tizniti, M.; Canosa, A.; Sims, I. R.; Smith, I. W. M. *Science* **2010**, *328*, 1258.
(23) Speranza, M. *J. Phys. Chem.* **1998**, *102*, 7535.
(24) Murray, C.; Derro, E. L.; Sechler, T. D.; Lester, M. I. *J. Phys. Chem. A* **2007**, *111*, 4727.
(25) Derro, E. L.; Sechler, T. D.; Murray, C.; Lester, M. I. *J. Chem. Phys.* **2008**, *128*, 244313.
(26) Mathisen, K. B.; Siegbahn, P. E. M. *Chem. Phys.* **1984**, *90*, 225.
(27) Dupuis, M.; Fitzgerald, G.; Hammond, B.; Lester, W. A. Jr.; Schaefer, H. F. III. *J. Chem. Phys.* **1986**, *84*, 2691.
(28) Varandas, A. J. C.; Yu, H. G. *Mol. Phys.* **1997**, *91*, 301.
(29) Setokuchi, O.; Sato, M.; Matuzawa, S. *J. Phys. Chem. A* **2000**, *104*, 3204.
(30) Yu, H. G.; Varandas, A. J. C. *Chem. Phys. Lett.* **2001**, *334*, 173.
(31) Fabian, W. M. F.; Kalcher, J.; Janoschek, R. *Theor. Chem. Acc.* **2005**, *114*, 182.
(32) Braams, B. J.; Yu, H. *Phys. Chem. Chem. Phys.* **2008**, *10*, 3150.
(33) Anglada, J. M.; Olivella, S.; Solé, A. *J. Chem. Theory Comput.* **2010**, *6*, 2743.
(34) Blint, R. J.; Newton, M. D. *J. Chem. Phys.* **1973**, *59*, 6220.
(35) Varandas, A. J. C. *Int. Rev. Phys. Chem.* **2000**, *19*, 199.
(36) Mills, I. M. In *Molecular Spectroscopy: Modern Research*; Rao, N., Mathews, C., Eds.; Academic Press: New York, 1972; p 115.
(37) Truhlar, D. G. *J. Comput. Chem.* **1991**, *32*, 266.
(38) Schuurman, M. S.; Muir, S. R.; Allen, W. D.; Schaefer, H. F. III. *J. Chem. Phys.* **2004**, *120*, 11586.
(39) Tajti, A.; Csaszar, A. G.; Kallay, M.; Gauss, J.; Valeev, E. F.; Flowers, B. A.; Vazquez, J.; Stanton, J. F. *J. Chem. Phys.* **2004**, *121*, 11599.
(40) Goldman, N.; Leforrestier, C.; Saykally, R. J. *J. Phys. Chem. A* **2004**, *108*, 787.
(41) Schenter, G. K.; Kathmannn, S. M.; Garrett, B. C. *J. Phys. Chem. A* **2002**, *106*, 1557.
(42) Kendall, R. A.; Dunning, T. H. Jr.; Harrison, R. J. *J. Chem. Phys.* **1992**, *96*, 6796.
(43) Woon, D. E.; Dunning, T. H. Jr. *J. Chem. Phys.* **1995**, *103*, 4572.

(44) Basis sets were obtained from the Extensible Computational Chemistry Environment Basis Set Database, version 02/25/04, as developed and distributed by the Molecular Science Computing Facility, Environmental and Molecular Sciences Laboratory, which is part of the Pacific Northwest Laboratory, P.O. Box 999, Richland, Washington 99352, USA, and funded by the U.S. Department of Energy. The Pacific Northwest Laboratory is a multiprogram laboratory operated by Battelle Memorial Institute for the U.S. Department of Energy under contract DE-AC06-76RLO 1830. Contact Karen Schuchardt for further information.
(45) Knowles, P. J.; Werner, H. J. *Chem. Phys. Lett.* **1988**, *145*, 514.
(46) Werner, H. J.; Knowles, P. J. *J. Chem. Phys.* **1988**, *89*, 5803.
(47) The partition is in this context especially meaningful when the CAS part of the total energy does not contain any significant fraction of the dynamical correlation, which should be the case when the active space coincides with the FVCAS one.
(48) Karton, A.; Martin, J. M. L. *Theor. Chem. Acc.* **2006**, *115*, 330.
(49) Jensen, F. *Theor. Chem. Acc.* **2005**, *113*, 267.
(50) Varandas, A. J. C. *J. Chem. Phys.* **2007**, *126*, 244105.
(51) Feller, D. *J. Chem. Phys.* **1992**, *96*, 6104.
(52) Feller, D. *J. Chem. Phys.* **1993**, *98*, 7059.
(53) Varandas, A. J. C. *J. Chem. Phys.* **2000**, *113*, 8880.
(54) Varandas, A. J. C. *J. Chem. Phys.* **2007**, *127*, 114316.
(55) Varandas, A. J. C. *J. Chem. Phys.* **2008**, *129*, 234103.
(56) Varandas, A. J. C. *J. Phys. Chem. A* **2008**, *112*, 1841.
(57) Varandas, A. J. C. *Theor. Chem. Acc.* **2008**, *119*, 511.
(58) Varandas, A. J. C. *J. Phys. Chem. A* **2010**, *114*, 8505.
(59) The use of C6 in MRCI-C6 should not be confused with the symbol +Q for the Davidson correction or the leading dispersion coefficient, implying instead[13] that core effects are neglected (C0 if they are fully considered). Similarly, the symbol +Q in CCSD(T)-C0+Q should not be confused with the Davidson correction, indicating that the effect of triple and quadruple excitations (with a VTZ basis) has been included[20] (cf. second and third colums of fourth entry in Table 1 of this reference).
(60) Spline fits are used in all plots to help visual perception, which may explain some differences that are observed for the dashed curves of this particular plot between 2.5 and 3.0 Å but which are not expected to occur in reality.
(61) Almlof, J.; Taylor, P. R. *J. Chem. Phys.* **1987**, *86*, 4070.
(62) Harding, L. B. *J. Phys. Chem.* **1991**, *95*, 8653.
(63) Kuhn, B.; Rizo, T. R.; Luckhaus, D.; Quack, M.; Suhm, M. A. *J. Chem. Phys.* **1999**, *111*, 2565.
(64) Pastrana, M. R.; Quintales, L. A. M.; Brandão, J.; Varandas, A. J. C. *J. Phys. Chem.* **1990**, *94*, 8073.
(65) Xu, C.; Xie, D.; Zhang, D. H.; Lin, S. Y.; Guo, H. *J. Chem. Phys.* **2005**, *122*, 244305.
(66) Babikov, D.; Kendrick, B. K.; Walker, R. B.; Pack, R. T.; Fleurat-Lesard, P.; Schinke, R. *J. Chem. Phys.* **2003**, *118*, 6298.
(67) Varandas, A. J. C. *THEOCHEM* **1988**, *166*, 59.
(68) Graff, M. M.; Wagner, A. F. *J. Chem. Phys.* **1990**, *92*, 2423.
(69) Let V_{ii} (i = 1, 2) be two diabatic potentials that intersect at a given geometry and V_{12} be the coupling potential that attains there its maximum interaction. If V_{11} is chemically bound but dissociates to products in an excited state and V_{22} is a repulsive curve that dissociates to ground-state products (the zero of energy), the resulting adiabatic potentials assume the following well-known form: $V_{\pm} = {}^1/_2(V_{11} + V_{22}) \pm {}^1/_2((V_{11} - V_{22})^2 + 4V_{12}^2)^{1/2}$. Of the two adiabatic potentials, V_- shows a maximum, after which it approaches the asymptote for ground-state products from below in typical cases where long-range attractive forces are present in the repulsive diabat. Thus, with the exception of cases where the crossing occurs in the attractive vdW part of the repulsive diabat, such a maximum is expected to lie above the zero of energy. In turn, V_+ shows typically a broad minimum and dissociates to the excited state products. A well studied diatomic which is representative of this situation is the classic ionic−covalent interaction in LiF[80] where the maximum is even absent due to the avoided intersection occurring far away in the long-range tail of the repulsive diabat. Consider now that there is a single state with a single stationary point (minimum) as for the title system, with the curve being characterized by covalent bonding at short-range, while at long-range electrostatic forces become dominant. For convenience, we may still think of the problem as if two states that avoid intersecting each other are involved. However, because both hypothetical diabats (V_{11} and V_{22}) dissociate to the same set of products but governed by forces with a distinct directionality, a simple analysis shows that the point of crossing must occur below (or at most at an energy identical to) the dissociation asymptote. Of course, it is assumed that the calculations do not suffer from BSSE or any other artifact that may invalidate the analysis.
(70) Huber, K. P.; Herzberg, G. *Molecular Spectra and Molecular Structure IV. Constants of Diatomic Molecules*; Van Nostrand: New York, 1979.
(71) Michels, H. H. *Adv. Chem. Phys.* **1981**, *45*, 225.
(72) Varandas, A. J. C.; Voronin, A. I. *J. Phys. Chem.* **1995**, *99*, 15846.
(73) At the *ab initio* level, force calculations for OH($X^2\Pi$) with the AVQZ basis at the HF, CAS, and MRCI levels of theory yield values of 4054.82, 3659.91, and 3741.82 cm^{-1}. Corresponding calculations for $O_2(X^3\Sigma_g^-)$ give 2008.53, 1547.69, and 1582.76 cm^{-1}. These values are to be compared with the experimental ones[70] of 3737.76_1 and 1580.19_3 cm^{-1}, respectively. The predicted equilibrium geometries at the same levels of theory are in the above order of 0.94968, 0.97337, and 0.97038Å for OH, while for O_2 they read 1.15086, 1.21538, and 1.20913 Å. The corresponding experimental values are[70] 0.96966 Å and 1.20752 Å.
(74) Jensen, F. *Introduction to Computational Chemistry*, 2nd ed.; Wiley: Chichester, U. K., 2006.
(75) Shavitt, I. *Mol. Phys.* **1998**, *94*, 3.
(76) Varandas, A. J. C. *Mol. Phys.* **1987**, *60*, 527.
(77) Chu, X.; Dalgarno, A. *J. Chem. Phys.* **2004**, *121*, 4083.
(78) Margoliash, D. J.; Meath, W. J. *J. Chem. Phys.* **1978**, *68*, 1426.
(79) Vydrov, O. A.; Voorhis, T. V. *Phys. Rev. A* **2010**, *81*, 062708.
(80) Varandas, A. J. C. *J. Chem. Phys.* **2009**, *131*, 124128.